Building and Environment 102 (2016) 39–53

Contents lists available at ScienceDirect

Building and Environment

journal homepage: www.elsevier.com/locate/buildenv

Visual assessment of contaminant impacts in multizone buildings

S.T. Parker [a, *], S. Williamson [a, b]

[a] Dstl, Porton Down, Salisbury, Wiltshire SP4 0JQ, United Kingdom
[b] Department of Oceanography, University of Hawai'i at Mānoa, United States

ARTICLE INFO

Article history:
Received 28 December 2015
Received in revised form
29 February 2016
Accepted 9 March 2016
Available online 15 March 2016

Keywords:
State-space
Multizone models
Exposure assessment
Air quality
Impact matrix

ABSTRACT

A novel method is presented for the visualisation of steady-state concentrations and exposures that may result from the indoor release of hazardous airborne material. This impact matrix approach is designed for the analysis of air flow results for multizone building models and is intended to complement existing multizone software. The matrices are derived from a state-space formulation and can be used to directly calculate steady-state concentrations for continuous constant release rates, or exposures for finite mass releases. In addition to steady-state conditions, methods to visualise the time dependence of concentration and exposure are also provided. Example matrices are calculated and visualised for a single residential dwelling, an apartment block and a commercial healthcare building. The resulting impact matrices are interpreted to derive system level information on the spread of airborne material within the buildings. The results show important differences between the buildings that depend on their connectivity and ventilation.

1. Introduction

1.1. Motivation

Building simulation is a key tool in assessing the impact of hazardous airborne releases within buildings. In some cases the location and characteristics of airborne contaminant sources are well known in advance, but in others, such as deliberate terrorist attack or accidental release, there may be a wide range of possible source locations and different time profiles of the mass released. Traditional approaches for studying such releases involve the simulation of a small set of scenarios and the resulting analysis can be limited in scope. This work aims to provide a complementary method to evaluate the impacts from a wide range of release locations and to enhance the understanding of contaminant transport.

An alternative approach for the analysis of hazardous releases in whole buildings has been developed for use with multizone models. The method considers internal dispersion under steady flow conditions and uses a visual representation of the normalised steady-state concentrations for all potential release locations within the building. It can also be shown that the same quantities relate to the maximum integrated concentrations, or exposures, for finite duration releases of a given mass. These quantities can be used to understand the impact of indoor airborne releases on air quality as well as directly relating them to human health effects. As an additional benefit, the method provides a system level perspective on the building and its ventilation that may have a much wider application.

1.2. Background

Multizone models such as CONTAM [1] and COMIS [2] are a class of building simulation tools that predict air flows and concentrations of airborne contaminants throughout multiple zones within a building. Multizone models cannot provide detailed predictions of air flows within rooms that are available from computational fluid dynamics (CFD) methods. However, they can make predictions of zone averaged concentrations and have the advantage that they can be applied to whole buildings because of their moderate execution times. In addition, they do not require the high level of specific information on geometry and boundary conditions required by CFD models. They have also been subject to a number of validation studies including [3,4] that have included comparison of air flow and contaminant concentrations. Multizone models provide considerable additional detail when compared to simple single zone indoor models that are used in some situations [5]. They have

* Corresponding author.
E-mail addresses: stparker@dstl.gov.uk (S.T. Parker), sarahw4@hawaii.edu (S. Williamson).

http://dx.doi.org/10.1016/j.buildenv.2016.03.007

been applied to a wide range of studies including indoor air quality [6,7], environmental tobacco smoke [8,9], spread of infectious disease [10,11] and monitoring and detection [12–14]. The numerical solution of contaminant transport within multizone models has also developed recently with the inclusion of additional solver options [15]. A useful overview of multizone and other indoor modelling methods can be found in Refs. [16,17].

Multizone models can be used to simulate single scenarios or a range of cases in turn. The results of these calculations are typically presented as time series plots of concentration for a given scenario or sometimes using coloured floor plans showing the spatial distribution of concentrations at a given time, or for a series of times [18]. However, a method to visually compare a range of release locations is not readily available. This paper sets out new methods for the visualisation of the resulting concentrations and exposures for multiple release locations and release profiles simultaneously. The use of integral solutions allows exposure to be assessed and compared for different locations without the explicit solution of concentration time series for specific release profiles. The method is not intended to replace CONTAM or the CONTAM results viewer, but aims to complement them by providing a concise, information-rich format to assist analysis and provide insight.

The methods take advantage of a state-space approach. State-space methods have become increasingly popular for building simulation studies. Yan et al. used these methods to model the emission of VOCs from building materials [19]. Wang et al. [20] applied state-space methods within a CFD framework to explore contaminant transport. State-space methods have also been used to study the control of temperature in three zones [21] and in multizone buildings [22], as well as for the detection of contaminant release events [23] and for studying the transport and dispersion of particles [24].

These previous studies demonstrate the flexibility and power of the approach. This work uses the formulation developed by Ref. [25] as a basis, because it allows the representation of many of the contaminant transport processes included within CONTAM. The same formulation has been extended and applied to the ingress of external contaminants in Ref. [26] and the solution of the resulting equations has been explored in Ref. [27]. The visualisation of contaminant transport using the state-space method was briefly introduced in Ref. [28], illustrating the potential for considering many release locations at the same time, a process which is not straightforward using other methods. This paper develops the theoretical basis for the visualisation methods and extends them, followed by demonstration of their use for three contrasting multizone building models.

2. Methodology

2.1. Theory

2.1.1. Assumptions

The multizone modelling approach [29,1] assumes that a building can be represented as a series of interconnected well-mixed zones. The analysis developed below also assumes that the air flow within the building is constant over the period of analysis. This assumption is consistent with the approach used within multizone models, which assume a quasi-static situation. This assumption may break down when the building is strongly influenced by meteorological conditions or for a mechanically ventilated building when there are sudden changes to the operation of the ventilation system. In such situations a series of steady states may be used.

2.1.2. Steady-state concentration

The change in internal concentration within a multizone building for a given air flow condition can be described by the state-space approach outlined in Refs. [25,26]. The governing equation for a multizone building with n zones can be written as

$$\dot{\mathbf{x}} = \mathbf{A}\mathbf{x} + \mathbf{B}\mathbf{u}, \tag{1}$$

where $\mathbf{x} = [x_1 x_2 \ldots x_n]^{\mathrm{T}}$ and x_i is the concentration in zone i [kg m^{-3}]; $\mathbf{A}$ is the n-by-n state matrix [s^{-1}]; $\mathbf{B}$ is an n-by-n matrix accounting for the dilution of sources by the zone volumes [m^{-3}] and $\mathbf{u}$ is an n-by-1 vector describing contaminant inputs into the system [kg s^{-1}]. The state matrix describes the interactions between the zones due to air flow and also takes into account losses within zones and those due to transfer between zones. A full description of the state-space formulation can be found in Ref. [25].

When there is a continuous source of contaminants released at a constant rate, a steady-state concentration distribution, $\mathbf{x} = \mathbf{x}_{\mathrm{ss}}$, can be determined when $\dot{\mathbf{x}} = 0$. Substituting into (1) gives

$$\mathbf{x}_{\mathrm{ss}} = -\mathbf{A}^{-1}\mathbf{B}\mathbf{u}. \tag{2}$$

Where $\mathbf{x}_{\mathrm{ss}}$ is a column vector describing the steady-state concentration in each zone resulting from the release defined by the input vector $\mathbf{u}$.

The input vector can represent both external concentrations affecting the building and internal releases. For the purposes of this paper only internal sources are considered and $\mathbf{u} = \mathbf{u}_{\mathrm{int}}$. The internal source term vector, $\mathbf{u}_{\mathrm{int}}$, is defined as $\mathbf{u}_{\mathrm{int}} = [s_1 s_2 \ldots s_n]^{\mathrm{T}}$, where s_i is the source strength in zone i [kg s^{-1}].

If the case with a source in only one zone, j, is considered then $s_i = 0$ for $i \neq j$ and $s_i = r$ for $i = j$, where r is the release rate [kg s^{-1}]. For convenience we define a dimensionless n-by-1 source location vector, $\mathbf{u}_{\mathrm{dl}}(j)$, where $\mathbf{u}_{\mathrm{dl}}(j)_i = 0$ if $i \neq j$ and $\mathbf{u}_{\mathrm{dl}}(j)_i = 1$ if $i = j$. Therefore, $\mathbf{u}_{\mathrm{int}} = \mathbf{u}_{\mathrm{dl}}(j)r$ and by substituting into (2) the steady state concentration vector, $\mathbf{x}_{\mathrm{ss}}(j)$, for a release in a single zone, j, can be written as

$$\mathbf{x}_{\mathrm{ss}}(j) = -\mathbf{A}^{-1}\mathbf{B}\mathbf{u}_{\mathrm{dl}}(j)r. \tag{3}$$

It is straightforward to calculate the steady-state concentration from a release in each zone in turn by appending column vectors of $\mathbf{u}_{\mathrm{dl}}(j)$, where $j = 1..n$ to give

$$\mathrm{X}_{ss} = -\mathbf{A}^{-1}\mathbf{B}\mathbf{U}_{dl}r, \tag{4}$$

where $\mathbf{X}_{\mathrm{ss}}$ is an n-by-n matrix and $X_{\mathrm{ss}i,j}$ is the steady state concentration in zone i resulting from a continuous release of strength r in zone j and

$$\mathbf{U}_{\mathrm{dl}} = \begin{bmatrix} 1 & 0 & \cdots & 0 \\ 0 & 1 & \ddots & \vdots \\ \vdots & \ddots & \ddots & 0 \\ 0 & \cdots & 0 & 1 \end{bmatrix}. \tag{5}$$

It is clear that $\mathbf{U}_{\mathrm{dl}}$ is simply the identity matrix and therefore

$$\mathbf{X}_{\mathrm{ss}} = -\mathbf{A}^{-1}\mathbf{B}r. \tag{6}$$

We define the impact matrix $\mathbf{M} = r^{-1}\mathbf{X}_{\mathrm{ss}}$ by dividing the concentration matrix by the release rate and note that $\mathbf{M}$ has units of [m^{-3} s]. The impact matrix can then be calculated as

$$\mathbf{M} = -\mathbf{A}^{-1}\mathbf{B}. \tag{7}$$

The impact matrix, $\mathbf{M}$, summarises the distribution of normalised steady-state concentrations resulting from a continuous

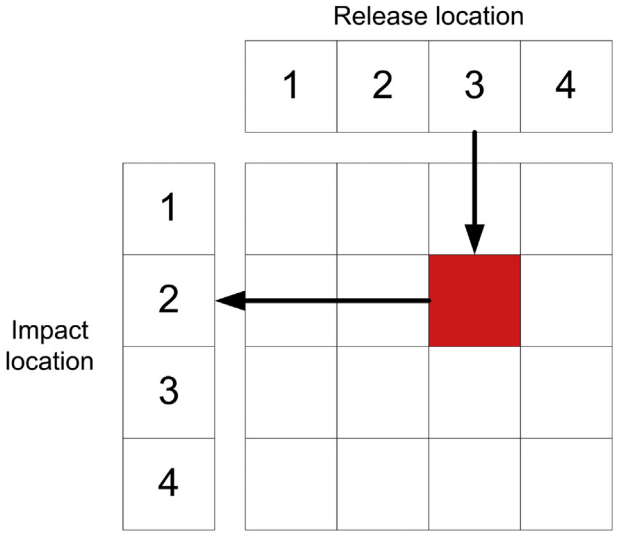

Fig. 1. Impact matrix interpretation for a simple four zone model. The colour value in the red square shows the steady-state concentration in zone 2 that would result from a continuous, constant release in zone 3, divided by the release rate. All entries of a full matrix are coloured to show all combinations of release and impact locations and a colour scale is used to allow quantitative interpretation. (For interpretation of the references to colour in this figure legend, the reader is referred to the web version of this article.)

release in every location in turn. Entry $M_{i,j}$ gives the steady-state concentration in zone i, divided by the release rate, resulting from a continuous release in zone j. The interpretation of the impact and release locations in the impact matrix is illustrated in Fig. 1 for a simple four zone case. The steady-state concentrations for a particular release rate are easily determined by multiplying **M** by the constant release rate, r.

The contents of the matrix can be plotted with a colour scale to give an overview of the steady-state concentration that will result from releases in different locations in the building. Example matrices are presented in Section 3.1 below.

2.1.3. Exposure

Although the steady-state concentration is useful for building analysis, in many cases the integrated concentration or cumulative exposure of building occupants is of particular interest as it can be related to the likelihood of health impacts. The cumulative exposure, $e_i(t)$ [kg m^{-3} s], for occupants within zone i, from time 0 to time t, is defined as

$$e_i(t) = \int_0^t x_i(s)\mathrm{d}s, \tag{8}$$

where t [s] is the time at the end of the exposure and s is a variable of integration.

The vector of exposures in each zone is defined as $\mathbf{e} = [\,e_1 e_2 \ldots e_n\,]^{\mathrm{T}}$ and can be written as

$$\mathbf{e}(t) = \int_0^t \mathbf{x}(s)\mathrm{d}s. \tag{9}$$

The governing differential equation (1) can be integrated [26] to give

$$\mathbf{x}(t) = e^{\mathbf{A}t}\mathbf{x}(0) + e^{\mathbf{A}t}\int_0^t e^{-\mathbf{A}\tau}\mathbf{B}(\tau)\mathbf{u}(\tau)\mathrm{d}\tau, \tag{10}$$

where τ is a variable of integration.

Substituting (10) into (9) gives

$$\mathbf{e}(t) = \int_0^t e^{\mathbf{A}s}\mathbf{x}(0)\mathrm{d}s + \int_0^t e^{\mathbf{A}s}\int_0^s e^{-\mathbf{A}\tau}\mathbf{B}(\tau)\mathbf{u}(\tau)\mathrm{d}\tau\mathrm{d}s, \tag{11}$$

where $\mathbf{x}(0)$ is the vector of zone concentrations at $t = 0$.

By exchanging the order of integration of the second term and noting that **B** is constant, the following expression can be derived [26]

$$\mathbf{e}(t) = \mathbf{A}^{-1}\left(e^{\mathbf{A}t} - \mathbf{I}\right)\mathbf{x}(0) + \mathbf{A}^{-1}\int_0^t \left(e^{\mathbf{A}(t-\tau)} - \mathbf{I}\right)\mathbf{B}\mathbf{u}(\tau)\mathrm{d}\tau. \tag{12}$$

It is of practical interest to consider the upper limit of the exposure in a given location for a given release of material. Ruling out the artificial case of zones that have no contaminant decay due to ventilation or other loss mechanisms, it can be shown that

$$\lim_{t\to\infty}\mathbf{e}(t) = -\mathbf{A}^{-1}\mathbf{x}(0) - \mathbf{A}^{-1}\mathbf{B}\int_0^\infty \mathbf{u}(\tau)\mathrm{d}\tau, \tag{13}$$

since all of the eigenvalues of **A** are strictly negative [26]. This property also guarantees that **A** has an inverse.

If only internal sources are considered then $\mathbf{u}(t) = \mathbf{u}_{\mathrm{int}}(t)$. Taking the case of zero initial concentrations in all zones and a single release of mass m in zone j, then $\mathbf{u}_{\mathrm{int}}(t) = \mathbf{u}_{\mathrm{dl}}(j)r(t)$, where $\mathbf{u}_{\mathrm{dl}}(j)$ is constant with time and

$$m = \int_0^\infty r(\tau)\mathrm{d}\tau. \tag{14}$$

In this case, the release rate, $r(t)$, is not constant and varies with time.

Substituting $\mathbf{u}_{\mathrm{int}}(t) = \mathbf{u}_{\mathrm{dl}}(j)r(t)$ into (13) and removing the constant term from the integral gives

$$\lim_{t\to\infty}\mathbf{e}(t) = -\mathbf{A}^{-1}\mathbf{B}\mathbf{u}_{\mathrm{dl}}(j)\int_0^\infty r(\tau)\mathrm{d}\tau. \tag{15}$$

Equation (14) can then be substituted into (15) to give an expression showing the upper limit for the exposure within each

Table 1
Building model details.

Model designation	Building type	Occupied floors	Zones	Internal volume	Fresh air change rate
DH-20	Residential detached	3	16	494 m^3	0.17 h^{-1}
APT-69	Residential apartment	6	56	1132 m^3	0.09 h^{-1}
Outpatients	Commercial healthcare	3	130	20,175 m^3	0.50 h^{-1}

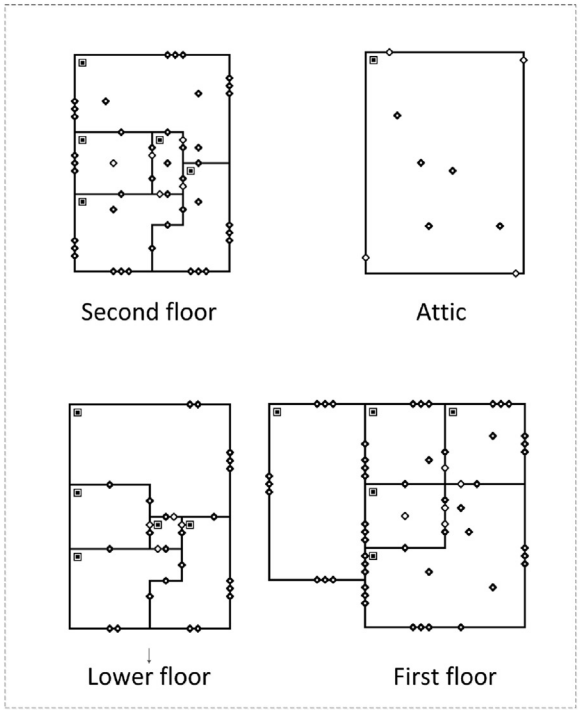

Residential detached house, DH-20

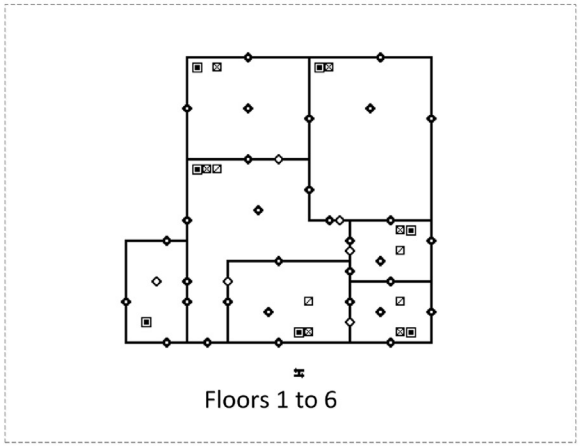

Residential apartment, APT-69

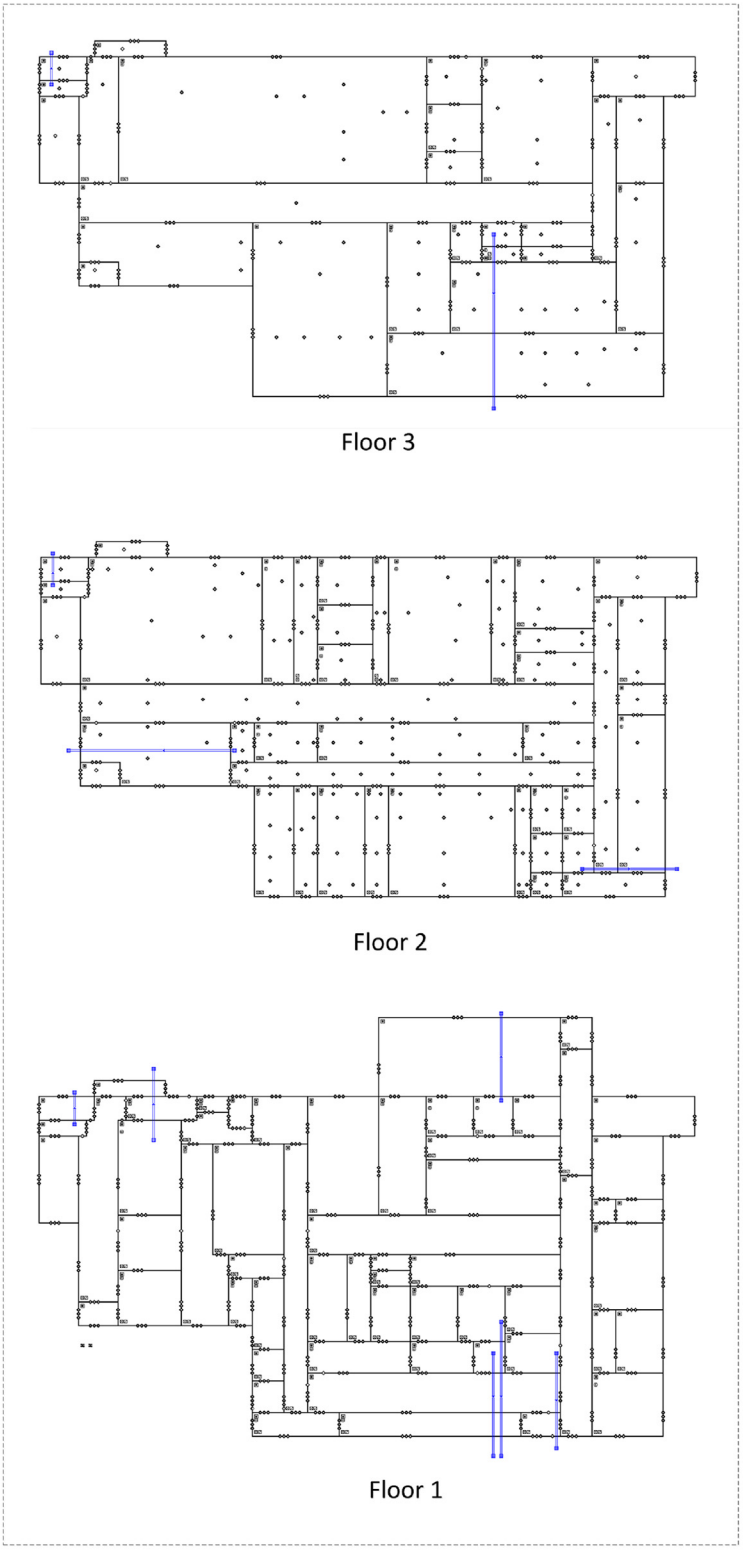

Commercial healthcare, outpatients

Fig. 2. Building model floor plans as represented in CONTAM (not to scale).

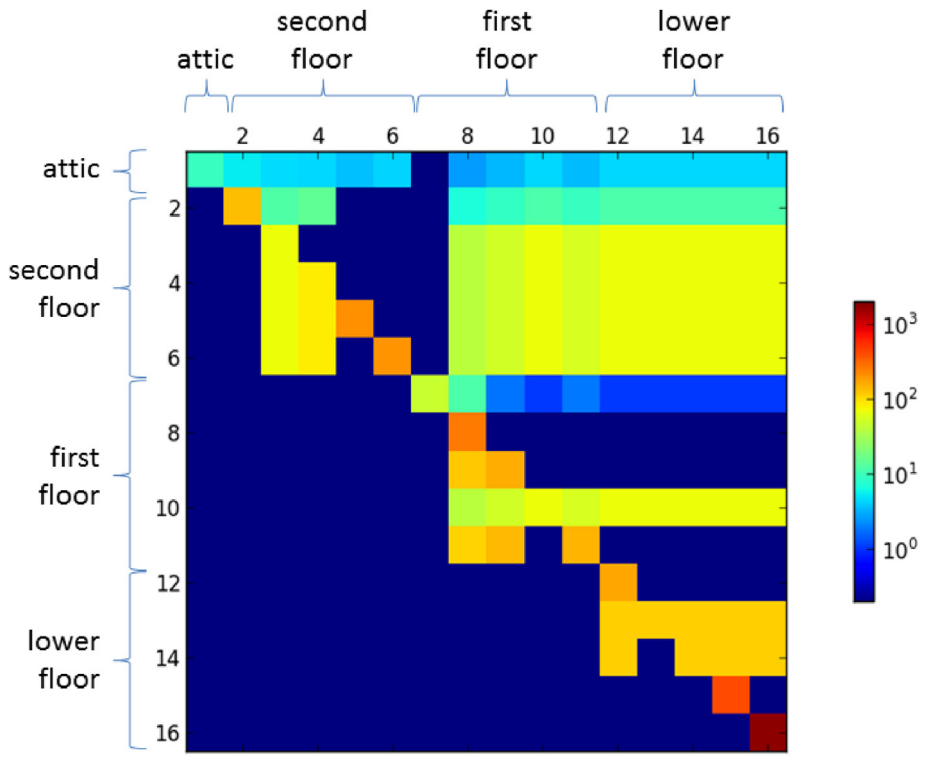

Fig. 3. Impact matrix for residential detached house, DH-20. Release zone shown by column label and impact zone by row label. Colour scale from 0.2 m^{-3} s to 2000 m^{-3} s. (For interpretation of the references to colour in this figure legend, the reader is referred to the web version of this article.)

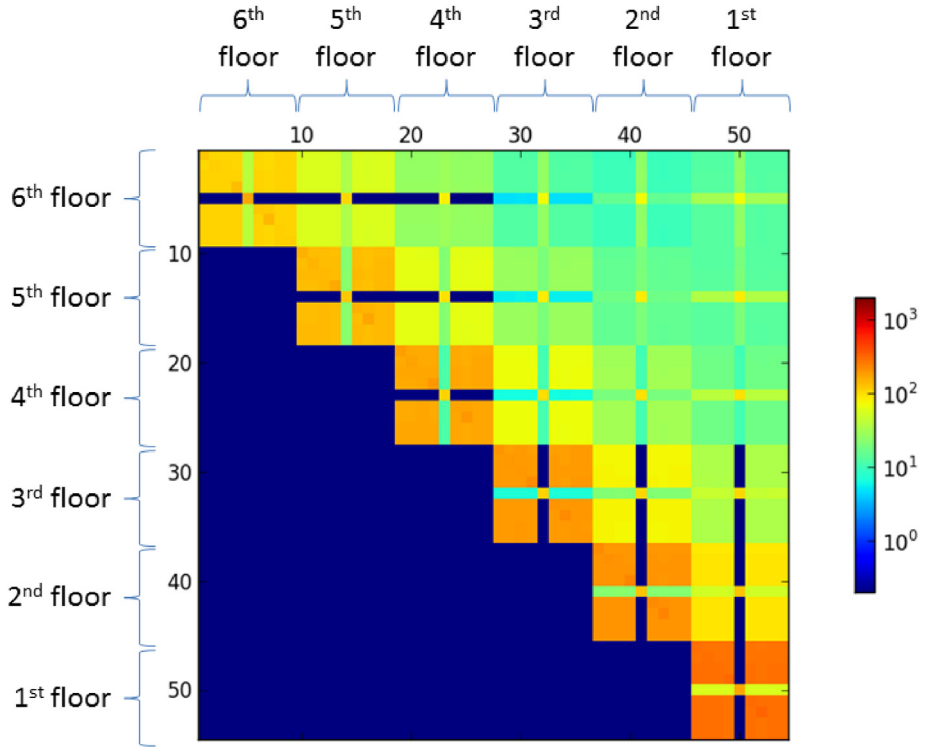

Fig. 4. Impact matrix for residential apartment, APT-69. Release zone shown by column label and impact zone by row label. Colour scale from 0.2 m^{-3} s to 2000 m^{-3} s. (For interpretation of the references to colour in this figure legend, the reader is referred to the web version of this article.)

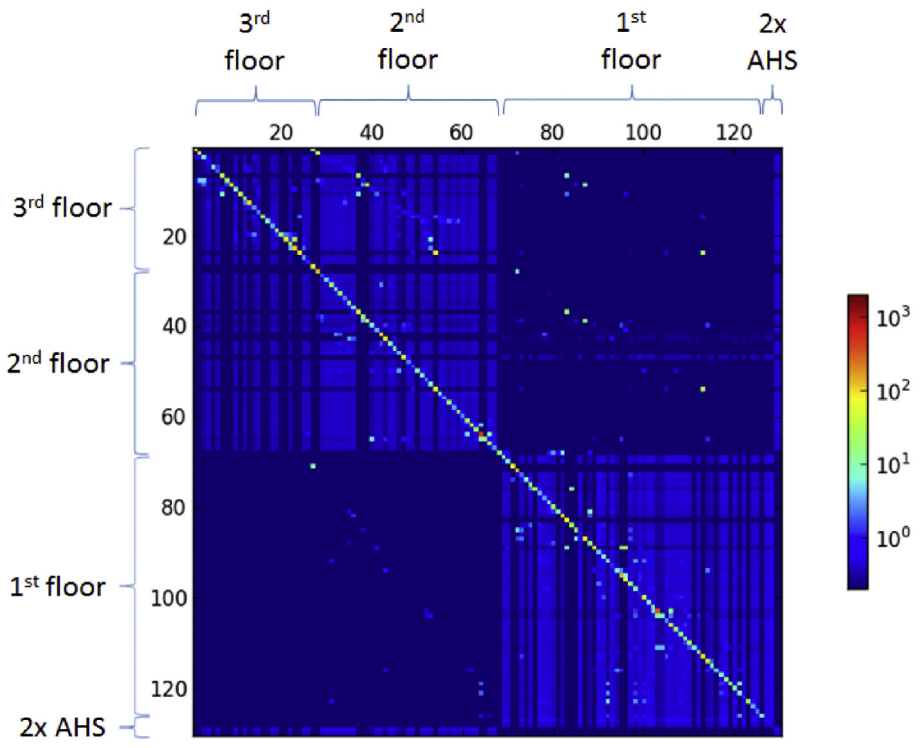

(a) Colour scale from $0.2\,\mathrm{m}^{-3}\,\mathrm{s}$ to $2000\,\mathrm{m}^{-3}\,\mathrm{s}$

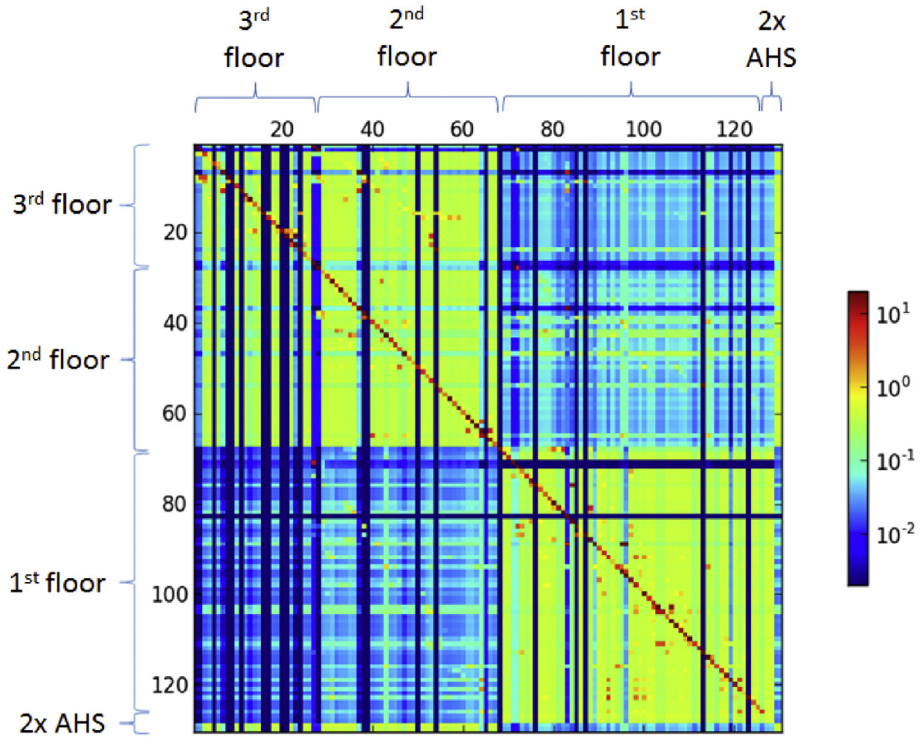

(b) Colour scale from $0.002\,\mathrm{m}^{-3}\,\mathrm{s}$ to $20\,\mathrm{m}^{-3}\,\mathrm{s}$

Fig. 5. Impact matrices for commercial healthcare outpatients building using two colour scales. Release zone shown by column label and impact zone by row label. (For interpretation of the references to colour in this figure legend, the reader is referred to the web version of this article.)

zone as a result of a release in zone j,

$$\lim_{t\to\infty} \mathbf{e}(t) = -\mathbf{A}^{-1}\mathbf{B}\mathbf{u}_{\mathrm{dl}}(j)m. \tag{16}$$

It is interesting to note that this exposure is not dependent on the release rate, only on the total mass released.

In the same way as for the steady-state concentrations, column vectors for each release zone can be appended to give the following result

$$\lim_{t\to\infty} \mathbf{E}(t) = -\mathbf{A}^{-1}\mathbf{B}m, \tag{17}$$

where $\mathbf{E}(t)$ is an n-by-n matrix and $E(t)_{i,j}$ is the exposure at time t, in zone i resulting from a release of mass m in zone j. Comparing (17) with (7) shows that the upper limit of the exposure matrix normalised by the release mass is also given by the impact matrix, $\mathbf{M}$,

$$m^{-1}\lim_{t\to\infty} \mathbf{E}(t) = -\mathbf{A}^{-1}\mathbf{B} = \mathbf{M}. \tag{18}$$

The impact matrix $\mathbf{M}$ therefore also summarises the distribution of limiting exposures resulting from a finite release mass in each location in turn. Entry $M_{i,j}$ can be interpreted as the upper limit on the exposure received within zone i, divided by the release mass, as a result of a finite release in zone j. Importantly, this value is independent of the variation of the release rate and only depends on the release mass and its location. The actual upper exposure limits can be determined by multiplying the impact matrix by the release mass of interest. The impact matrix can be considered as a representation of the relative normalised exposures for every combination of release and exposure zone.

It should be noted that the upper limit of the exposure may overestimate a building occupant's exposure when they remain within the zone for only a short time, or when the contaminant is released over a long period. A building occupant who moves between zones will receive a different exposure and may, in principle, receive an exposure higher than any of the zone-specific upper limits.

2.1.4. Time-resolved impact matrices

The impact matrix, $\mathbf{M}$, defined above has great utility as a screening tool to consider the upper limit on exposures resulting from different release masses. However, in some cases it is important to consider the shorter term variation in concentration and exposure. The state-space formulation can be applied to calculate the concentration and exposure at different times using equations (10) and (12).

By sacrificing some of the generality of the impact matrix considered above, the impact of an instantaneous release of mass, m, in any zone j can be considered. In that case the initial zone averaged concentration, $\mathbf{x}(0)_i = m/V_i$ when $i = j$ and $\mathbf{x}(0)_i = 0$ when $i \neq j$, where V_i is the volume of zone i. The initial concentration vector can be written as

$$\mathbf{x}(0) = \mathbf{V}^{-1}\mathbf{u}_{\mathrm{dl}}(j)m, \tag{19}$$

where $\mathbf{V}$ is a diagonal n-by-n matrix with $V_{i,i} = V_i$.

Substituting (19) into (10) and noting that $\mathbf{u} = 0$ gives

$$\mathbf{x}(t) = e^{\mathbf{A}t}\mathbf{V}^{-1}\mathbf{u}_{\mathrm{dl}}(j)m. \tag{20}$$

Using the same approach as before and noting that $\mathbf{B} = \mathbf{V}^{-1}$ [25], the concentration at time t, resulting from an instantaneous release in each zone can be calculated as

$$\mathbf{X}(t) = e^{\mathbf{A}t}\mathbf{B}m, \tag{21}$$

where $X(t)_{i,j}$ is the concentration in zone i resulting from an instantaneous release of mass m in zone j.

The time-resolved impact matrix for concentration, $\mathbf{M}_{\mathrm{TR,C}}(t)$ [m^{-3}], is defined as the time-resolved concentration matrix normalised by the release mass,

$$\mathbf{M}_{\mathrm{TR,C}}(t) = m^{-1}\mathbf{X}(t) = e^{\mathbf{A}t}\mathbf{B}. \tag{22}$$

Entry $\mathbf{M}_{\mathrm{TR,C}}(t)_{i,j}$ gives the concentration in zone i at time t, divided by the release mass, resulting from an instantaneous release in zone j.

Similarly, a time-resolved impact matrix for exposure, $\mathbf{M}_{\mathrm{TR,E}}(t)$ [m^{-3} s], can be defined as the time-resolved exposure matrix normalised by the release mass. Using equation (12) as a starting point this can be calculated as

$$\mathbf{M}_{\mathrm{TR,E}}(t) = m^{-1}\mathbf{E}(t) = \mathbf{A}^{-1}\left(e^{\mathbf{A}t} - \mathbf{I}\right)\mathbf{B}. \tag{23}$$

Entry $\mathbf{M}_{\mathrm{TR,E}}(t)_{i,j}$ gives the exposure in zone i at time t, divided by the release mass, resulting from an instantaneous release in zone j.

2.2. Multizone modelling

2.2.1. Multizone software

The multizone software CONTAM v3.1 (National Institute of Standards and Technology, (NIST)) [1] was used to simulate the air flow through three buildings under steady-state conditions with constant internal and external temperatures. The resulting air flows were used for each building in order to illustrate the use of the impact matrix approach.

2.2.2. Building models

Three different building models were chosen to cover a range of building features (Table 1). Two residential buildings, a three-storey detached house (DH-20) and a six-storey apartment building (APT-69), were selected were selected from a collection of multizone models for US residential stock [30]. The detached house included no mechanical ventilation, while the apartment building was served by a purely recirculating mechanical ventilation system for each floor and exhaust fans in the kitchen and bathroom of each apartment. Although the CONTAM model includes 56 zones, the two zones representing the exhaust fan air handling system are not represented in the impact matrix as the exhaust fans were not operational during the simulation. The internal temperature was 23 °C for all zones for the residential buildings as defined in the provided building models [30].

A three-storey healthcare building was selected from a smaller collection of multizone models for US commercial buildings [6]. The building model represents an outpatients healthcare clinic containing rooms with a range of functions. The building is served by two mechanical ventilation systems, with one system serving the first floor and the other serving the second and third floors. The internal temperature was 20 °C for all zones in this building as defined in the provided building model [6].

Building model floor plans are shown in Fig. 2 which illustrate the relative arrangement of the zones. All building models included permeable walls and ceilings. Flows between zones were typically represented by cracks beneath closed doors or open doors modelled as one-way flows with a powerlaw model. The resulting steady-state air flows reflect the model representations and environmental conditions. It might be expected that a two-way representation of open doors would result in a different impact matrix.

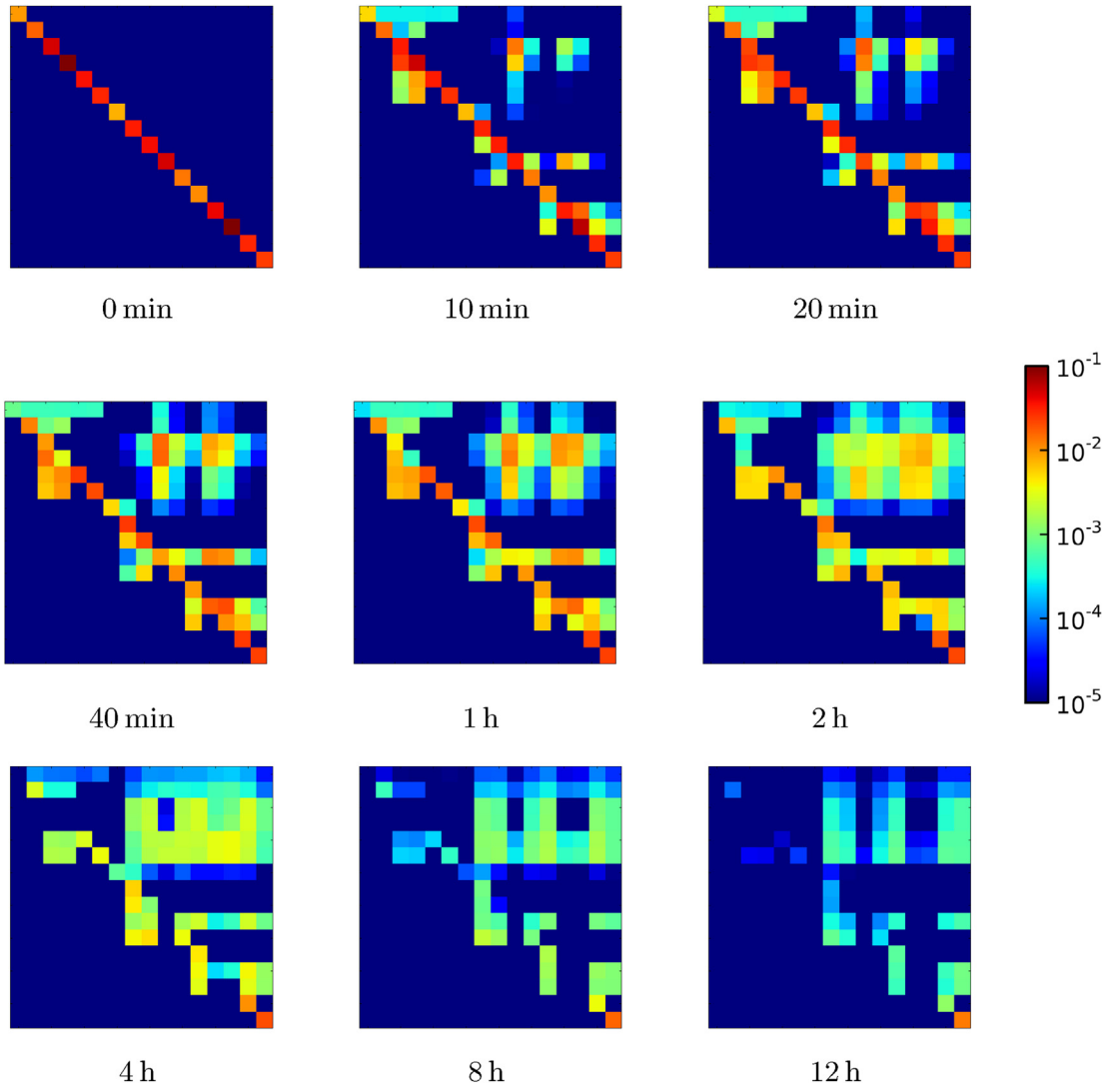

Fig. 6. Time-resolved impact matrix for concentration, $\mathbf{M}_{TR,C}(t)$ for various times. Residential detached house, DH-20 building. Zone order is the same as shown in Fig. 3. Colour scale from 1×10^{-5} m^{-3} to 1×10^{-1} m^{-3}. (For interpretation of the references to colour in this figure legend, the reader is referred to the web version of this article.)

This highlights another potential use of the impact matrix approach in examining the importance of model specification choices. Full details of the building models can be found in Refs. [6,30].

2.2.3. Environmental conditions

A single set of meteorological conditions was used to calculate the building air flows for all three buildings. The following parameters were chosen: wind speed 3.28 m s^{-1} at 10 m height, wind direction from 0°, external temperature 20 °C and atmospheric pressure 101,325 Pa. The values were chosen were purely for demonstration purposes and should be not be interpreted as typical values. All other building model parameters were left as the default values from Refs. [6,30].

2.2.4. Impact matrix calculation

The steady-state airflows calculated by CONTAM were used together with the zone volumes to create state-space representations of each building. In particular, this allowed the definition of the matrices **A** and **B** used for the calculation of the impact matrices, following the formulation in Ref. [25]. For the example cases here, no losses due to penetration, filtration or surface interaction were included. However, these effects can be accounted for using this visualisation method by including their effect in the governing matrices.

For example, the definition of **A** from Ref. [25], allows losses due to deposition and attenuation within each zone and filtration or other losses during passage between zones to be included. Because these factors are combined with the flows after the air flow solution, the effect of different loss rates can be rapidly assessed and compared. The transport and dispersion represented by the example visualisations in this work may be considered to be representative of an inert tracer gas or non-reactive pollutant such as carbon dioxide. The formulation of the impact matrices is normalised to the release rate for the steady-state concentration, or the release mass for the limiting exposure, and so applies to a wide range of release rates. However, there is an implicit assumption that the contaminant is sufficiently dilute that its density does not modify its transport and dispersion.

The derivation of the state-space matrices and matrix algebra were performed using the Python™ programming language (Python v 2.7.4) [31] and the Numerical Python (NumPy v 1.7.1) [32] and Scientific Python (SciPy v 0.12.0) [33] libraries. The CONTAM

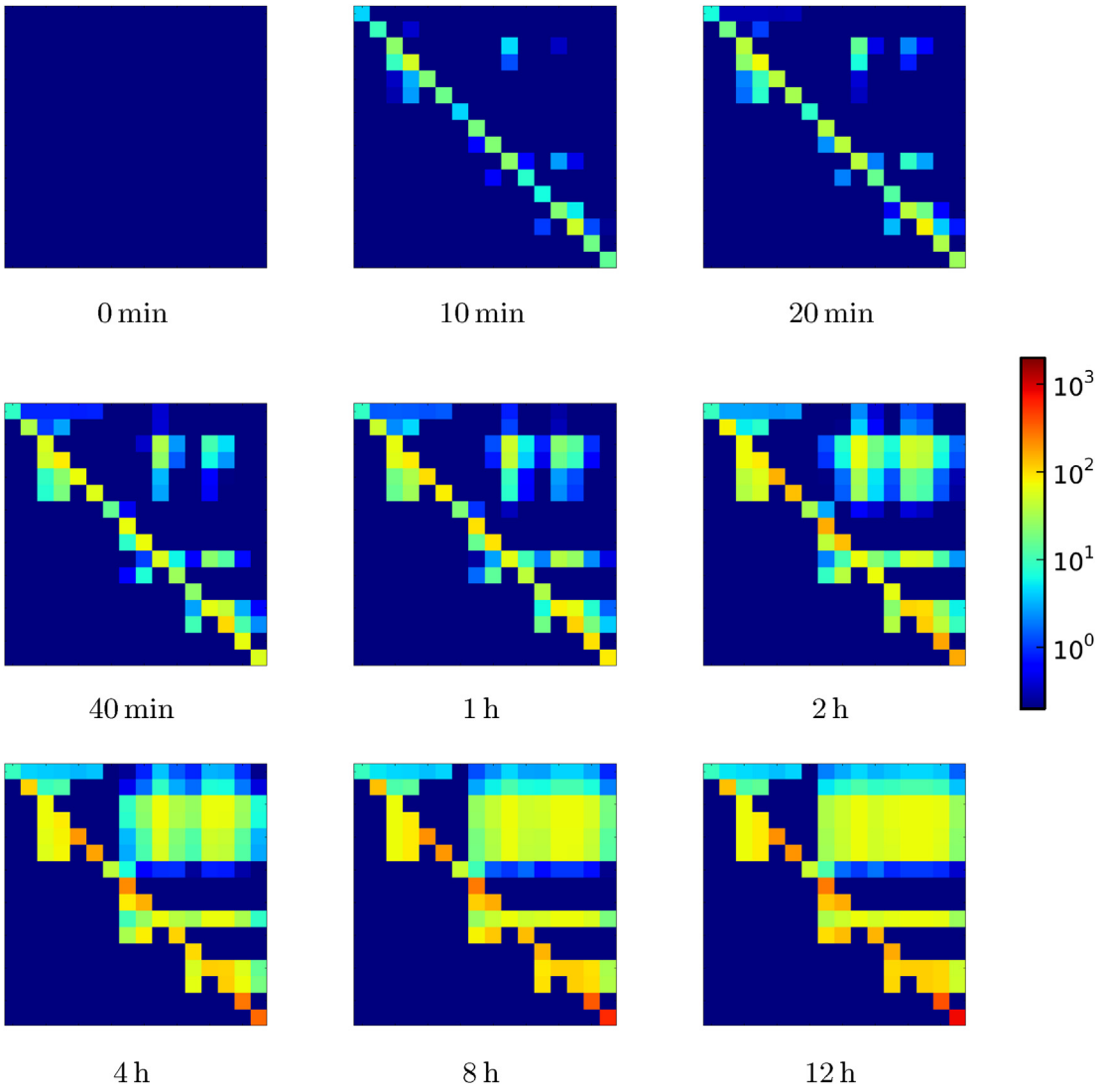

Fig. 7. Time-resolved impact matrix for exposure, $\mathbf{M}_{TR,E}(t)$ for various times. Residential detached house, DH-20 building. Zone order is the same as shown in Fig. 3. Colour scale from 0.2 m^{-3} s to 2000m^{-3} s. (For interpretation of the references to colour in this figure legend, the reader is referred to the web version of this article.)

airflows were read from a link flow result file produced by the CONTAM Simread3 tool using a Python™. This information was combined with information extracted from the CONTAM project file to produce the required matrices. The impact matrix images were created using the Matplotlib (Matplotlib v 1.2.1) library [34].

3. Results and discussion

This section presents example impact matrices calculated for the three building models. The impact matrices represent only a single meteorological condition and should be considered as illustrative only.

3.1. Impact matrices

3.1.1. Residential detached house, DH-20

Fig. 3 shows the impact matrix calculated for the detached house model. The matrix is indexed by the number of the release zone on the horizontal and impact zone on the vertical. It is worth noting that CONTAM begins zone numbering at the top of the building so the upper-left of the impact matrix represents releases towards the top of the building, with zone numbers to the lower-right indicating a lower location in the building. For this building, zone 1 is the attic space, zones 2 to 6 are on the second floor, zones 7 to 11 are on the first floor and 12 to 16 are on the lower floor.

Interpreting the matrix, it can be seen that, for the simulated air flow conditions, a release in the attic space (zone 1, the first column) has no impact on any other zone. For this air flow condition, releases do not affect floors below the release floor. This is a result of the temperature difference between the interior (23 °C) and exterior (20 °C) causing a positive stack flow in the building. It can also be seen that releases on the first and lower floor affect all of the zones in the second floor and attic. Zone 7 on the first floor is an exception as this is the garage with no floor above. Although not shown here, variation in wind direction influences the transfer between zones within floors and the appearance of the impact matrix.

3.1.2. Residential apartment, APT-69

Fig. 4 shows the impact matrix for the residential apartment building. The matrix shows a clear division into six blocks on the diagonal. Each block represents an apartment, with the top floor to

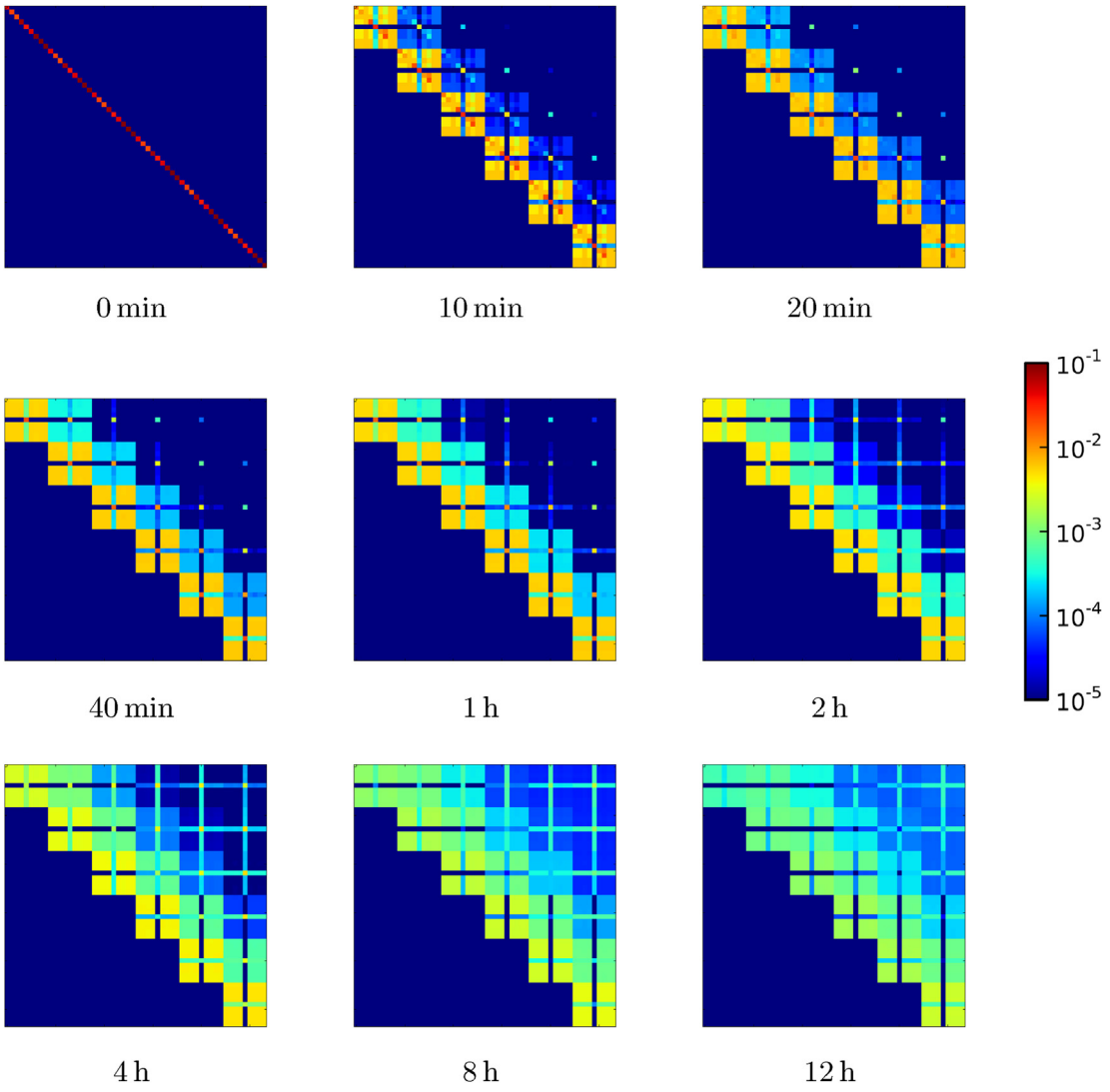

Fig. 8. Time-resolved impact matrix for concentration, $\mathbf{M}_{TR,C}(t)$ for various times. Residential apartment building, APT-69. Zone order is the same as shown in Fig. 4. Colour scale from 1×10^{-5} m^{-3} to 1×10^{-1} m^{-3}. (For interpretation of the references to colour in this figure legend, the reader is referred to the web version of this article.)

the upper-left (zones 1 to 9). The central zone within each block represents the stairwell zone.

Interpreting the matrix, it can be seen that a release within an apartment, other than in the stairwell, affects the whole apartment. This is a result of the separate recirculating ventilation system serving each apartment. The impact matrix value (referred to hereafter as the impact) is slightly higher in the lower apartments because of lower fresh air change rates due to lower stack-driven differential pressures. In common with the detached house building, there is a net transfer of material up through the building due to a positive stack effect. For example, material released in the lowest apartment (zones 46 to 54) rises up through the building affecting the apartments above.

The behaviour of a release in the stairwells (zones 5, 14, 23, 32, 41, 50) is more complex. For the stairwell zones serving the three lowest floors, the predicted air flow through the small closed door crack is one-way only and flows out of the apartment into the stairwell. For the stairwell zones serving the three highest floors, this flow direction is reversed with air flowing from the stairwell zone into the apartment on that floor. As a result, a release in the lowest stairwell (zone 50) does not affect the three lower floor apartments, but does affect the upper apartments. For a larger opening a two-way flow might be expected and the resulting impact matrix would differ.

3.1.3. *Commercial healthcare, outpatients*

Fig. 5 shows the impact matrix for the commercial outpatients healthcare building. The figure shows the impact matrix with two different colour scales. In Fig. 5 (a) the same colour scale used for the previous two buildings has been applied to allow comparison between the buildings. However, the volumetric fresh air flow rates are higher for this building due to the larger building volume and slightly higher fresh air change rate. As a result, the impact matrix values are considerably lower. Fig. 5 (b) shows the same matrix with a scale that is 100 times lower and allows easier interpretation.

Interpreting the matrix, it is clear that there are two regions with higher impact present as blocks on the diagonal. Although these are of approximately equal size, the upper-left block (zones 1 to 67) represents the upper two floors, served by one air handling system, and the lower-right block (zones 68 to 126) represents the lower floor, served by a single air handling system. Zones 127 to 130

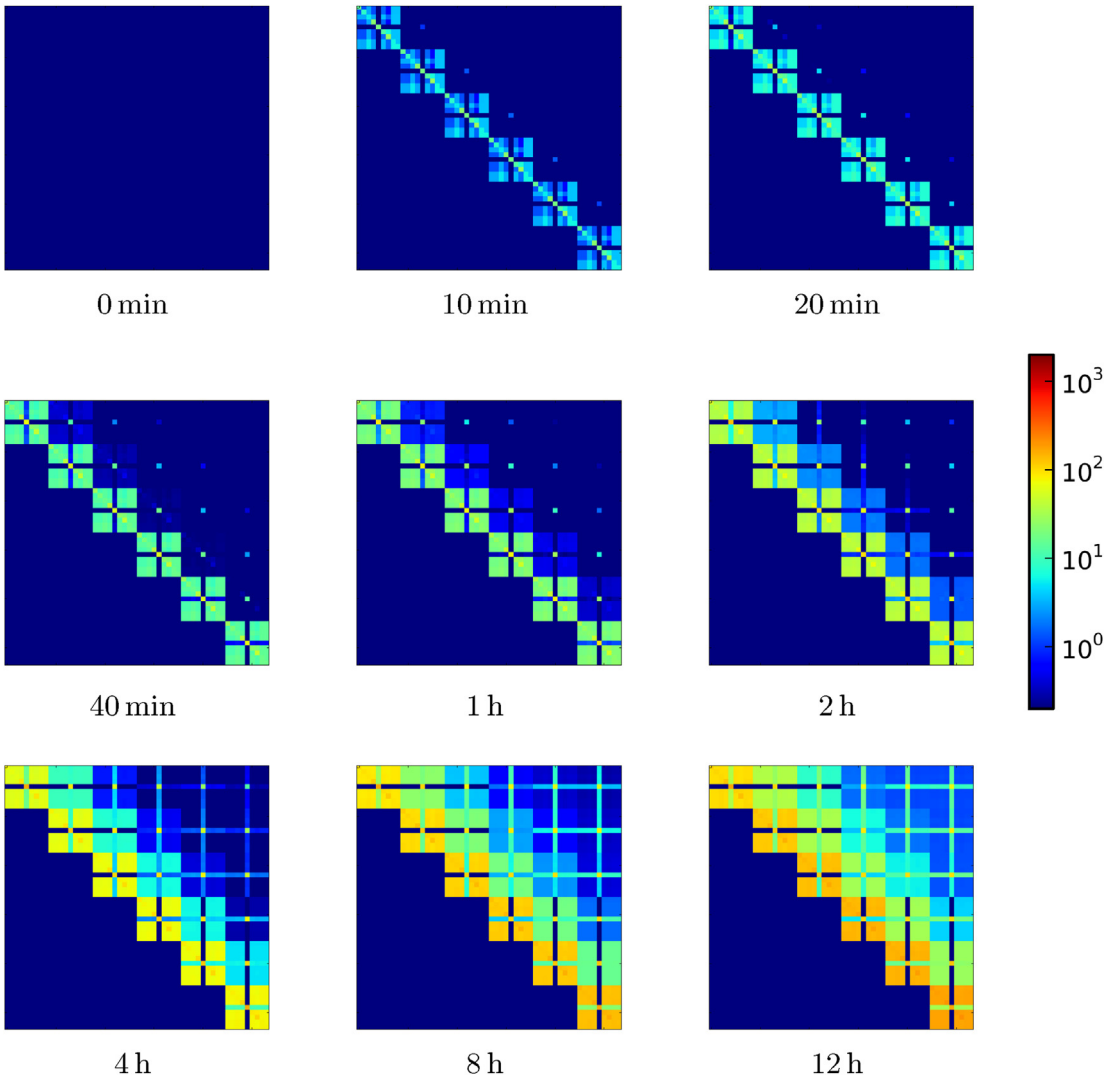

Fig. 9. Time-resolved impact matrix for exposure, $\mathbf{M}_{TR,E}(t)$ for various times. Residential apartment building, APT-69. Zone order is the same as shown in Fig. 4. Colour scale from 0.2 m^{-3} s to 2000m^{-3} s. (For interpretation of the references to colour in this figure legend, the reader is referred to the web version of this article.)

represent the two air handling systems serving all floors.

The diagonal stands out clearly for this building, indicating that the impact within the release zone is higher than the impact in surrounding zones. This effect can be seen to a lesser extent in the other buildings. It is more pronounced in this case because of the dilution in the mechanical ventilation system which distributes airborne material to the other zones served by the system. For those other zones, the impact is reasonably uniform. There is some transfer between floors and air handling system zones for this building. As expected, there is no evidence of a strong stack effect for this air flow condition in this building since there is a much higher ventilation rate and the internal and external temperatures are the same.

The impact matrix in Fig. 5 (b) is also characterised by some clear dark blue vertical lines. These correspond to zones with direct exhaust routes, either through leakage paths or ducted ventilation. Releases in these zones affect the release zone but do not affect any other zones in the building. There are also a small number of horizontal lines of dark blue. These correspond to zones pressurised by external wind and not served by the mechanical ventilation system. As a result contaminants released in other zones do not reach these zones.

Although the main objective of this work is to demonstrate the use of the impact matrix visualisation methods, it is interesting to consider briefly the potential implications of the results for indoor air quality for this building. Under the ventilation conditions examined here it is clear that contaminant sources have the largest impact in the release zone. There is likely to be lower level exposure in the zones that are served by the same air handling system with the remainder of the zones within the building experiencing a lower level of exposure still. This type of analysis may prove useful when combined with a consideration of contaminant sources, a wider range of ventilation conditions and other factors that may influence indoor air quality. Similar behaviour may also be expected for other mechanically ventilated commercial buildings.

3.2. Time-resolved impact matrices

3.2.1. Residential detached house, DH-20

Fig. 6 shows the time-resolved impact matrices for concentration for the detached house building, DH-20. The initial concentration shows high values on the diagonal, corresponding to the release zones. The actual values depend on the zone volumes. With increasing time, values in other zones change colour as material

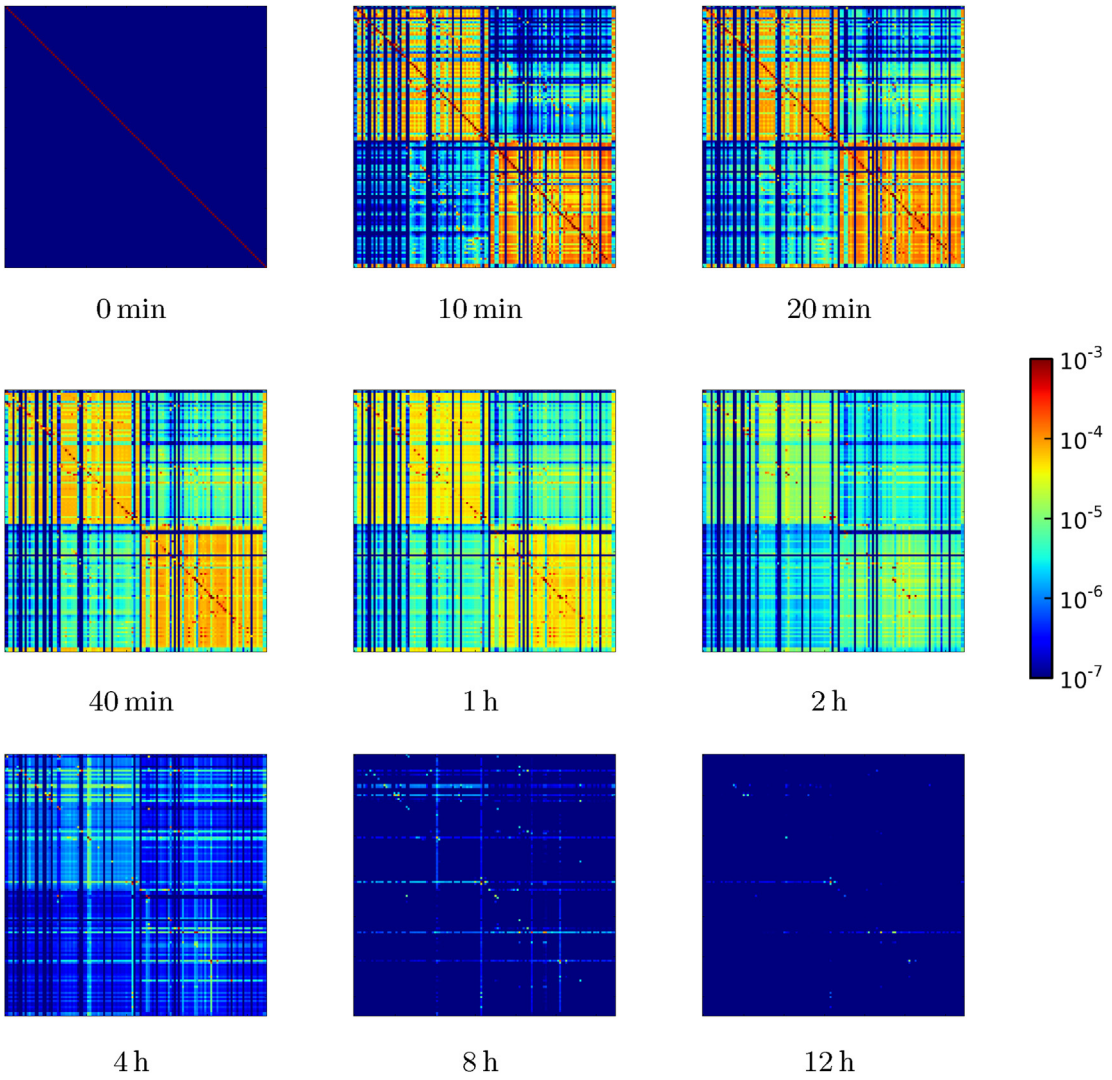

Fig. 10. Time-resolved impact matrix for concentration, $\mathbf{M}_{TR,C}(t)$ for various times. Commercial healthcare outpatients building. Zone order is the same as shown in Fig. 5. Colour scale from 1×10^{-7} m^{-3} to 1×10^{-3} m^{-3}. (For interpretation of the references to colour in this figure legend, the reader is referred to the web version of this article.)

spreads through the building. Careful inspection shows that the attic (zone 1) is affected by releases on the upper floor. The upper floor is affected by zones 10 and 13, which correspond to the stairwell in the lower floor. Releases in other zones on the lower floors take longer to reach the upper floors. By 1 h the concentrations in some of the release zones have visibly reduced. By 12 h the highest concentrations remaining are those in the upper floors resulting from lower releases in the building.

Fig. 7 shows the time-resolved impact matrices for exposure for the detached house, DH-20. As expected from the time-resolved concentration matrices, the exposure builds up along the diagonal first, corresponding to the release zones. The exposure in the remainder of the building builds up more slowly over a period of hours.

3.2.2. Residential apartment, APT-69

Fig. 8 shows the time-resolved impact matrix for concentration for the residential apartment building, APT-69. From the initial high concentrations in the release zones, material rapidly spreads to the other zones in the apartment. However, there remains visible variation in concentration within the apartments for at least 20 min when viewed closely. By 40 min the concentrations appear uniform within the non-stairwell zones in each apartment. There is visible transport of contaminant to the floor above the release apartment from 10min. Concentrations are raised by transport via the stairwell into higher apartments from 40 min depending on the release zone. Because of the low fresh air change rate, concentrations remain raised even at 12 h.

Fig. 9 shows the time-resolved exposure matrix for the same building. It lags behind the time-resolved concentration matrix with the high initial concentrations in the release apartment affecting exposure most strongly at early times. It is interesting to note that even in the 12 h matrix, there is a slight increase in exposure in the release zones, on the diagonal, compared to the remainder of the apartment. This is also consistent with the original impact matrix (Fig. 4).

3.2.3. Commercial healthcare, outpatients

Fig. 10 shows the time-resolved impact matrices for concentration for the healthcare outpatients building. The colour scale is 100 times lower than that used for the other two buildings in order to show the variation of values. The initial concentrations are hard to determine because of the large number of zones. However, by 10 min the effect of the recirculating ventilation system can be seen

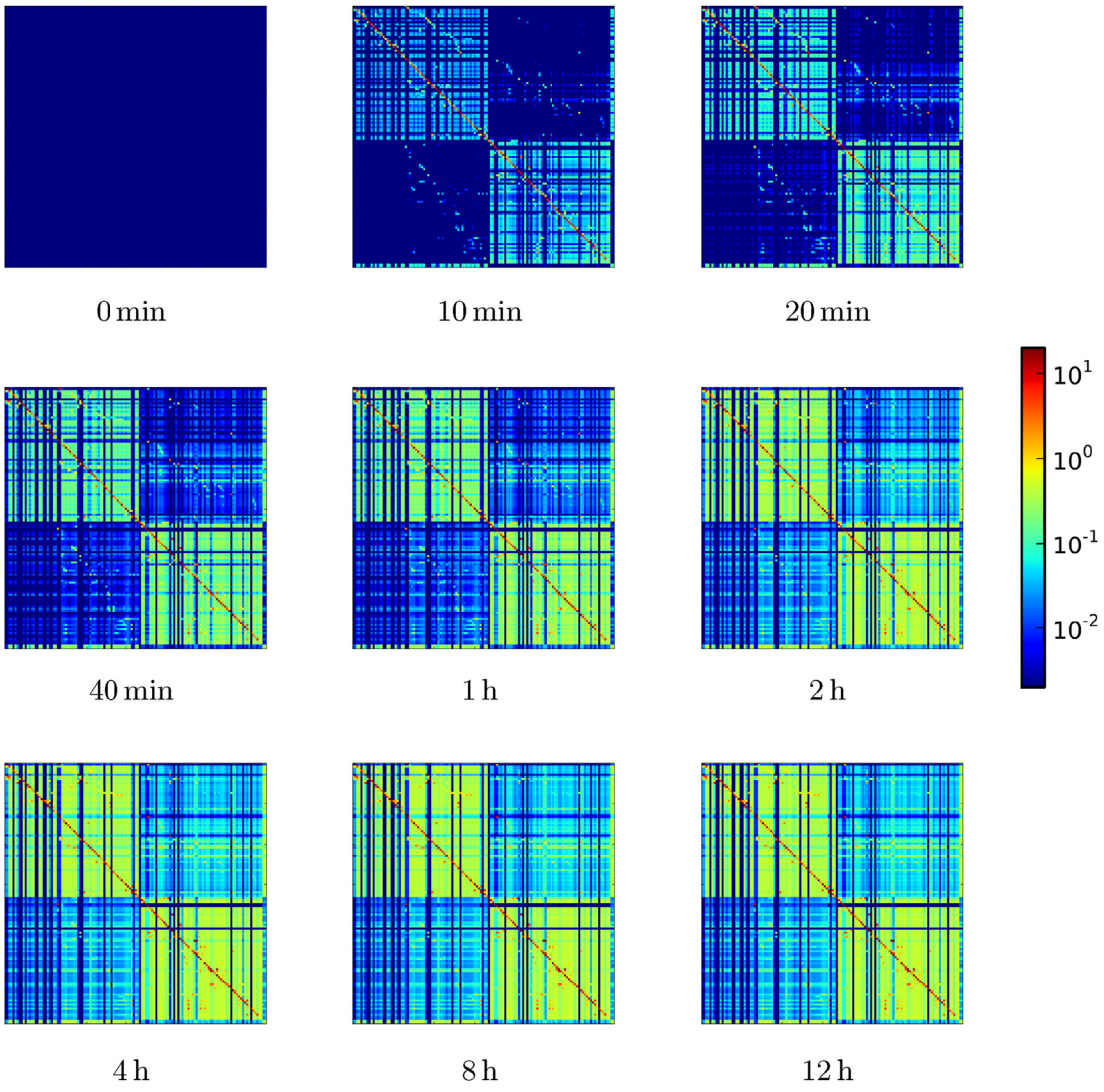

Fig. 11. Time-resolved impact matrix for exposure, $\mathbf{M}_{TR,E}(t)$ for various times. Commercial healthcare outpatients building. Zone order is the same as shown in Fig. 5. Colour scale from 0.002 m^{-3} s to 20 m^{-3} s. (For interpretation of the references to colour in this figure legend, the reader is referred to the web version of this article.)

clearly by the presence of two large blocks on the diagonal, with each block being served by a different air handling system. Some transfer to the other air handling zones and associated floor(s) can also be seen at this early time. The concentration in the ventilated spaces continues to rise until at least 20 min but starts to fall by 40 min. By the final 12 h matrix, the concentrations are below the lower end of the colour scale in all but a small number of release cases, associated with small zones lacking mechanical ventilation.

Fig. 11 shows the time-resolved impact matrices for exposure for the same building. The colour scale is 100 times lower than that used for the other two buildings in order to show the variation of values. As expected from the time-resolved concentration matrices, the release zone exposure increases rapidly. The exposure in the two main ventilation regions develops next, followed by the other floors. Because of the higher fresh air supply rate for this building, the exposure matrices show little change after 4 h. At that point the exposure in the release zones remains higher than that in the ventilated regions because of the dilution with external air.

3.3. Discussion

The impact matrices and time-resolved impact matrices provide a condensed form of information on steady-state building ventilation. Examining the resulting matrices for three contrasting buildings brings out a number of features. In particular, the range of values within the impact matrix reflects the total building fresh air flow rate, with higher matrix values resulting from lower fresh air flow rates. The fresh air flow rate is of course determined by the building volume and the fresh air change rate. The dependence on the fresh air flow rate can be appreciated by considering mass balance in a single zone model. In the absence of other loss rates, the steady-state concentration for a given continuous release can be shown to be inversely proportional to the fresh air flow rate into the space.

The pattern within the impact matrix provides information on the connectivity between zones and the organisation of the ventilation system(s). Whilst this information can be obtained by examining individual simulation results, the ability to view the impact of each release location at the same time allows the system behaviour to be observed.

The impact matrices provide information on the transport and ventilation under steady air flow conditions. The matrices can be interpreted as normalised steady-state concentration or exposure. In the former case it is important to recognise that such

concentrations may take some time to establish. The matrices can be calculated under a range of different building operation and meteorological conditions to examine their effect. The time-resolved impact matrices can also be used to assess whether the timescales of transport and dispersion will be shorter than the variation of the air flow conditions due to changes in ventilation operation or meteorology. If that is not the case then the variation of air flow conditions should be included in the simulation using traditional iterative solution methods. This may be particularly relevant for very leaky or draughty buildings, where sudden changes in meteorology or to door or window opening may cause rapid changes to the air flow. In these cases, the steady-state flow solution and impact matrix approach is unlikely to be as useful. For intermediate cases, the examination of the impact matrices for a series of different steady-state airflow conditions may be informative, even when an iterative solution may ultimately be required.

The brief examples explored here have compared the impact matrices for three different illustrative buildings. In addition, the impact matrix approach can readily be used to examine differences within the same building for different flow conditions. For example, the change resulting from different meteorological conditions can be examined or the change due to different mechanical ventilation settings. It can also provide a powerful tool for building ventilation design. In addition to designing ventilation to control contaminant sources within buildings, the approach may be valuable for thermal management for mechanically ventilated buildings, where temperatures do not strongly influence air flow.

The approach can also be used to examine the benefits of different mitigation strategies, such as the effect of filters with different properties. The influence of particle deposition can also be examined for particle phase materials or surface sorption for chemical materials. Although not shown here, the results can be combined with release masses and toxicological exposure thresholds to determine expected health impacts.

Interpreting the impact matrices requires the analyst to become familiar with this form of visualisation. In addition, a translation of the zone numbers to building locations is needed to make sense of the matrices. This can be achieved manually using the list of zones from CONTAM. For interactive use, the matrix can be presented in a form where the zone details are provided to the user as contextual information. Information on building floors and ventilation systems can also be provided either as fixed annotations or responsive contextual information.

4. Conclusions

A novel approach to the visualisation of the impact within buildings of internal airborne contaminant releases has been developed. The impact matrix approach uses steady-state air flows calculated by multizone models to estimate the steady-state concentrations resulting from continuous internal releases. The same information has also been shown to provide quantification of the limiting exposure from internal releases of finite duration. The approach presents information on all possible internal release locations simultaneously.

The time dependence of the impacts within buildings is addressed by the use of time-resolved impact matrices for both concentration and exposure. These matrices provide information on the spread of airborne material for a short duration release.

Impact matrices have been presented for three example multizone models, demonstrating the rapid identification of a number of features of interest. In addition to the provision of direct estimates of steady-state concentrations and exposures, the approach allows a system level assessment of the building space with many potential applications.

Acknowledgements

This work was made possible by the public availability of databases of multizone models for residential and commercial buildings from the National Institute of Standards and Technology, for which the authors are most grateful. Dr Parker was supported by the Dstl Research Scholarship scheme. The authors are also grateful to Dr David Lorenzetti for suggestions on the wider application of the impact matrix approach which have contributed to the discussion.

References

[1] G.N. Walton, W.S. Dols, CONTAM User Guide, Program Documentation, Technical Report NISTIR 7251, National Institute of Standards and Technology, 2010.
[2] A. Haas, A. Weber, V. Dorer, W. Keilholz, R. Pelletret, COMIS v3.1 simulation environment for multizone air flow and pollutant transport modelling, Energy Build. 34 (2002) 873–882.
[3] F. Haghighat, A.C. Megri, A comprehensive validation of two airflow models – COMIS and CONTAM, Indoor Air 6 (1996) 278–288.
[4] S.J. Emmerich, Validation of multizone IAQ modeling of residential-scale buildings: A review, Trans. Am. Soc. Heat. Refrig. Air Cond. Eng. 107 (2001) 619–628.
[5] F. Haghighat, H. Huang, Integrated IAQ model for prediction of VOC emissions from building material, Build. Environ. 38 (2003) 1007–1017.
[6] L.C. Ng, A. Musser, A. Persily, S.J. Emmerich, Airflow and Indoor Air Quality Models of DOE Reference Commercial Buildings, National Institute of Standards and Technology, 2012. Technical Report NIST TN1734.
[7] L.C. Ng, A.K. Persily, S.J. Emmerich, {IAQ} and energy impacts of ventilation strategies and building envelope airtightness in a big box retail building, Build. Environ. 92 (2015) 627–634.
[8] M.D. Sohn, D.M. Lorenzetti, Siting bio-samplers in buildings, Risk Anal. 27 (2007) 877–886.
[9] T.A. Myatt, T. Minegishi, J.G. Allen, D.L. MacIntosh, et al., Control of asthma triggers in indoor air with air cleaners: a modeling analysis, Environ. Health 7 (2008) b54.
[10] S.J. Emmerich, D. Heinzerling, J.-i. Choi, A.K. Persily, Multizone modeling of strategies to reduce the spread of airborne infectious agents in healthcare facilities, Build. Environ. 60 (2013) 105–115.
[11] I.T. Yu, Y. Li, T.W. Wong, W. Tam, A.T. Chan, J.H. Lee, D.Y. Leung, T. Ho, Evidence of airborne transmission of the severe acute respiratory syndrome virus, N. Engl. J. Med. 350 (2004) 1731–1739.
[12] Y.L. Chen, J. Wen, Sensor system design for building indoor air protection, Build. Environ. 43 (2008) 1278–1285.
[13] Y.L. Chen, J. Wen, Comparison of sensor systems designed using multizone, zonal, and CFD data for protection of indoor environments, Build. Environ. 45 (2010) 1061–1071.
[14] A. Bastani, F. Haghighat, J.A. Kozinski, Contaminant source identification within a building: Toward design of immune buildings, Build. Environ. 51 (2012) 320–329.
[15] D.M. Lorenzetti, W.S. Dols, A.K. Persily, M.D. Sohn, A stiff, variable time step transport solver for {CONTAM}, Build. Environ. 67 (2013) 260–264.
[16] Q. Chen, Ventilation performance prediction for buildings: A method overview and recent applications, Build. Environ. 44 (2009) 848–858.
[17] Q. Chen, K. Lee, S. Mazumdar, S. Poussou, L. Wang, M. Wang, Z. Zhang, Ventilation performance prediction for buildings: model assessment, Build. Environ. 45 (2010) 295–303.
[18] B. Polidoro, User Guide for NIST ContamRV (Contam Results Viewer) 3.0, 2011.
[19] W. Yan, Y. Zhang, X. Wang, Simulation of {VOC} emissions from building materials by using the state-space method, Build. Environ. 44 (2009) 471–478.
[20] X. Wang, F. Wang, C. Zhao, Characterizing transportation of indoor gaseous contaminant using the state space method, Build. Environ. 45 (2010) 2148–2159.
[21] Y. Yao, K. Yang, M. Huang, L. Wang, A state-space model for dynamic response of indoor air temperature and humidity, Build. Environ. 64 (2013) 26–37.
[22] J. Hu, P. Karava, A state-space modeling approach and multi-level optimization algorithm for predictive control of multi-zone buildings with mixed-mode cooling, Build. Environ. 80 (2014) 259–273.
[23] M. Michaelides, V. Reppa, M. Christodoulou, C. Panayiotou, M. Polycarpou, Contaminant event monitoring in multi-zone buildings using the state-space method, Build. Environ. 71 (2014) 140–152.

[24] S. Zhai, Z. Li, B. Zhao, State-space analysis of influencing factors on airborne particle concentration in aircraft cabins, Build. Environ. 74 (2014) 13–21.
[25] S.T. Parker, V.E. Bowman, State-space methods for calculating concentration dynamics in multizone buildings, Build. Environ. 46 (2011) 1567–1577.
[26] S. Parker, C. Coffey, J. Gravesen, J. Kirkpatrick, K. Ratcliffe, B. Lingard, J. Nally, Contaminant ingress into multizone buildings: an analytical state-space approach, Build. Simul. 7 (2014) 57–71.
[27] S.T. Parker, D.M. Lorenzetti, M.D. Sohn, Implementing state-space methods for multizone contaminant transport, Build. Environ. 71 (2014) 131–139.
[28] S. T. Parker, Contaminant transport in enclosed spaces – a state-space approach, Ventilation 2012 Conference, Paris, France, 2012.
[29] D. Lorenzetti, Computational aspects of nodal multizone airflow systems, Build. Environ. 37 (2002) 1083–1090.
[30] A. Persily, A. Musser, D. Leber, A Collection of Homes to Represent the U.S. Housing Stock, Technical Report NISTIR 7330, National Institute of Standards and Technology, 2006.
[31] D.M. Beazley, Python essential Reference, fourth ed., Addison-Wesley, Upper Saddle River, NJ, 2009.
[32] S. van der Walt, S. Colbert, G. Varoquaux, The NumPy array: a structure for efficient numerical computation, Comput. Sci. Eng. 13 (2011) 22–30.
[33] SciPy Community, SciPy Reference Guide Release 0.12.0, 2013.
[34] J.D. Hunter, Matplotlib: a 2D graphics environment, Comput. Sci. Eng. 9 (2007) 90–95.